ELSEVIER

Physica A 298 (2001) 56–68

PHYSICA A

www.elsevier.com/locate/physa

Cluster structure and dynamics in a mesoscopic solvent

Song Hi Lee[a], Raymond Kapral[b,*]

[a] *Department of Chemistry, Kyungsung University, Pusan 608-736, South Korea*
[b] *Chemical Physics Theory Group, Department of Chemistry, University of Toronto, Toronto, Canada M5S 3H6*

Abstract

The structural properties and dynamics of molecular clusters embedded in a mesoscopic solvent are investigated. The solvent interactions are taken into account through a multi-particle collision operator that conserves mass, momentum and energy and the solvent dynamics is updated at discrete time intervals. The cluster particles interact among themselves and with the solvent molecules through intermolecular forces. The properties of large and small Lennard–Jones clusters interacting with the mesoscopic solvent molecules through repulsive Lennard–Jones interactions are studied as a function of the potential parameters. Modifications of both the cluster and solvent structure as a result of solute–solvent interactions are considered. Since the solvent dynamics correctly reduces to that given by the hydrodynamic equations on long distance and time scales, the effects of hydrodynamic interactions on single and multi-particle diffusion are taken into account. © 2001 Elsevier Science B.V. All rights reserved.

PACS: 05.20.−y; 36.40.Sx; 61.46.+w

Keywords: Cluster; Pair correlation function; Hydrodynamic interactions

1. Introduction

In many instances, one is interested in the dynamical behavior of fluids on long distance and time scales and in such regimes a continuum description is appropriate. The use of the Navier–Stokes equations to describe fluid flow is a prime example of such a case. If macroscopic particles, such as large colloidal particles, are embedded in a continuum solvent, their dynamics and interactions are influenced by the

---

* Corresponding author. Tel.: +1-416-978-6106; fax: +1-416-978-5325.
E-mail address: rkapral@gatto.chem.utoronto.ca (R. Kapral).

PII: S0378-4371(01)00211-4

hydrodynamic properties of the medium. The hydrodynamic fields couple to the particles through boundary conditions at the surfaces of the particles [1,2]. Approaches of this type can be used to understand how Brownian particle dynamics is driven by hydrodynamic fields [3] and how hydrodynamic interactions contribute to the structure of the friction or diffusion tensors of the macroscopic particles [4–8].

When the solvent dynamics is not treated explicitly but its effect is accounted for in terms of frictional and random forces, the dynamics of embedded particles is described by Langevin equations of motion. In Langevin equation approaches of this type, often a position-dependent friction tensor is employed to account for hydrodynamic interactions among the particles.

Hydrodynamic approaches have also proved very successful in describing the dynamics of small molecules in solution [9]. For microscopic particles, there is considerable ambiguity concerning the nature of the boundary conditions that should be applied at the particle surface and, indeed, one should investigate the validity of these models in view of the microscopic space and time scales [10]. In addition, there are subtle features involved in the microscopic derivations of multi-particle Langevin descriptions of particle dynamics from the full evolution equations [11,12].

We have recently constructed a mesoscopic model for fluid dynamics [13]. In this model, which is a variant of direct simulation Monte Carlo (DSMC) [14,15], fluid particles interact through multi-particle collision events which take place at discrete time intervals. Between such collision events the particles undergo free streaming motion. The dynamics conserves mass, momentum and energy and yields the exact hydrodynamic equations of motion for the conserved fields on long distance and time scales. One may consider the dynamics of solute molecules in this mesoscopic solvent and because the solvent is described at an effective particle level the solute and solvent molecules interact through intermolecular forces rather than through boundary conditions. This leads to a hybrid description of the dynamics where solute molecules evolve by Newton's equations of motion but the solvent evolves through the multi-particle mesoscale dynamics [16].

Part of the utility of such a method is that motions of large molecular entities with nanometer length scales should be described in a physically meaningful fashion which accounts for the specific nature of the interactions with the solvent that occur on short scales and also takes into account the hydrodynamic solvent effects on the motion that occur on long scales. Both effects play important roles in conformational changes in large proteins and other biomolecules. An application of a variant of the hybrid MD scheme has been applied recently to a study of polymer dynamics [17].

In this paper, we consider the dynamics of Lennard–Jones clusters with sizes ranging from a few to over a 100 particles in order to investigate the dynamics of complex molecular entities in the mesoscopic solvent. Conditions are chosen so that the clusters persist in vacuum in liquid-like states for long time periods without evaporation. We then study the modifications in the cluster structure and dynamics when they are embedded in the mesoscale solvent. The intermolecular interactions with the solvent are varied to investigate how the cluster properties change.

The outline of the paper is as follows: Section 2 summarizes both the mesoscale fluid dynamics and the hybrid molecular dynamics–mesoscale solvent model. Section 3 presents results for the cluster dynamics in vacuum and in the mesoscale fluid solvent. Both small and large clusters are considered in order to explore different degrees of contact between the solvent and cluster molecules. Comparisons with continuum theories are made. The conclusions of the study are presented in Section 4.

2. Model for cluster dynamics in a mesoscopic solvent

The system we investigate comprises a cluster, whose particles interact through attractive intermolecular forces, embedded in a solvent whose dynamics is treated at a mesoscopic level. The solvent molecules labeled $1,\ldots,N$ have phase space coordinates $(\mathbf{r}^{(N)},\mathbf{v}^{(N)})=(\mathbf{r}_1,\mathbf{r}_2,\ldots,\mathbf{r}_N,\mathbf{v}_1,\mathbf{v}_2,\ldots,\mathbf{v}_N)$, while the cluster particles, labeled $N+1,\ldots,N+M$ have phase space coordinates $(\mathbf{r}^{(M)},\mathbf{v}^{(M)})=(\mathbf{r}_{N+1},\mathbf{r}_{N+2},\ldots,\mathbf{r}_{N+M},\mathbf{v}_{N+1},\mathbf{v}_{N+2},\ldots,\mathbf{v}_{N+M})$.

The total potential energy of the system is made up of cluster particle–cluster particle and cluster particle–solvent molecule interactions,

$$V(\mathbf{r}^{(M)},\mathbf{r}^{(N)})=V_{cc}(\mathbf{r}^{(M)})+V_{cs}(\mathbf{r}^{(M)},\mathbf{r}^{(N)})\,. \tag{1}$$

There are no solvent molecule–solvent molecule interactions since these are taken into account by multi-particle collisions in the mesosopic treatment of the solvent dynamics.

To carry out multi-particle solvent molecule collisions, the system is partitioned into cells and time is divided into discrete time intervals τ. At any time instant, a cell will contain a certain number of solvent molecules. At the discrete time instants, the solvent molecules undergo multi-particle collisions which are carried out in the following way: each cell is assigned at random a rotation operator $\hat{\omega}$ from a set of rotation operators, Ω. The velocity of each solvent molecule in the cell is rotated relative to the center of mass velocity of the molecules in the cell V by the rotation operator $\hat{\omega}$,

$$\mathbf{v}_i \to \mathsf{V}+\hat{\omega}[\mathbf{v}_i-\mathsf{V}]\,. \tag{2}$$

Such multi-particle collisions are carried out independently in each cell.

For times between the discrete time intervals at which solvent multi-particle collisions take place, all particles in the system, cluster particles and solvent molecules, evolve according to Newton's equations of motion,

$$\begin{aligned}\dot{\mathbf{x}}_i &= \mathbf{v}_i\,,\\ m_i\dot{\mathbf{v}}_i &= -\frac{\partial V}{\partial \mathbf{r}_i}=\mathbf{F}_i\,,\end{aligned} \tag{3}$$

where m_i is the mass of particle i and the potential energy V is that given in Eq. (1). If the solvent molecules are within the range of interaction of the solvent–cluster potential energy, then their dynamics is influenced by these interactions; otherwise they simply undergo free streaming motion.

In the absence of cluster particles, the mesoscale solvent dynamics is a variant of DSMC [14,15] with a modified collision rule. The multi-particle collision dynamics conserves the mass, momentum and energy in each cell. The phase space volume is preserved and the collision rule ensures that an equilibrium microcanonical ensemble distribution exists. The solvent dynamics can be compactly formulated in terms of the following kinetic equation for the phase space probability distribution function [13]:

$$P(\mathbf{v}^{(N)}, \mathbf{r}^{(N)} + \mathbf{v}^{(N)}, t + \tau) = \mathscr{C} P(\mathbf{v}^{(N)}, \mathbf{r}^{(N)}, t)\,, \tag{4}$$

where the collision operator $\mathscr{C}$ is given by

$$\begin{aligned} &\mathscr{C} P(\mathbf{v}^{(N)}, \mathbf{r}^{(N)}, t) \\ &\quad = \frac{1}{||\Omega||^L} \sum_{\Omega^L} \int d\check{\mathbf{v}}^{(N)} P(\check{\mathbf{v}}^{(N)}, \mathbf{r}^{(N)}, t) \prod_{i=1}^{N} \delta(\mathbf{v}_i - \mathsf{V}_\xi - \hat{\omega}_\xi[\check{\mathbf{v}}_i - \mathsf{V}_\xi])\,, \end{aligned} \tag{5}$$

and $\check{\mathbf{v}}^{(N)} = (\check{\mathbf{v}}_1, \check{\mathbf{v}}_2, \ldots, \check{\mathbf{v}}_N)$ denotes the set of pre-collision velocities and ξ is the coordinate of a coarse-grained cell of the system. From an analysis of this equation, we have shown that the mesoscopic solvent model correctly describes the hydrodynamics of the conserved variable fields [13].

2.1. *Simulation method*

Given the above description of the model, the system Hamiltonian is

$$H = \sum_i \frac{1}{2} m_i \mathbf{v}_i^2 + \sum_{i<j} V_{\alpha_i \alpha_j}(|\mathbf{r}_i - \mathbf{r}_j|)\,, \tag{6}$$

where $\alpha_i = c$ if i is a cluster particle and s if it is a solvent molecule. The cluster particles interact with each other via Lennard–Jones (LJ) potentials,

$$V_{cc} = 4\varepsilon_{cc} \left[\frac{\sigma_{cc}^{12}}{r^{12}} - \frac{\sigma_{cc}^{6}}{r^{6}} \right]\,, \tag{7}$$

while the cluster particle–solvent molecule interactions are repulsive and are given by truncated LJ potentials,

$$V_{cs}(r) = \begin{cases} 4\varepsilon_{cs}[\frac{\sigma_{cs}^{12}}{r^{12}} - \frac{\sigma_{cs}^{6}}{r^{6}} + \frac{1}{4}], & r \leqslant 2^{1/6}\sigma_{cs} \\ 0, & r > 2^{1/6}\sigma_{cs} \end{cases}\,. \tag{8}$$

The cluster particle–cluster particle interaction parameters are $\sigma_{cc} = 0.34$ nm and $\varepsilon_{cc} = 1.00604$ kJ/mol and the values for the cluster particle–solvent molecule interactions are $\varepsilon_{cs} = 1.00604$ kJ/mol with σ_{cs} taking either of two values, 0.17 or 0.221 nm. The masses of the cluster particles are $m_c = 39.948$ g/mol and the solvent molecules have masses $m_s = 3.9948$ g/mol.

The simulations were carried out in a cubic box of length $L = 5.44$ nm with periodic boundary conditions containing $N = 327\,680$ solvent molecules with number density $\rho_s = 2035.42\ \mathrm{nm}^{-3}$. Clusters with $M = 5$, 25 and 123 particles were studied. Newton's equations of motion were integrated using the velocity Verlet algorithm [18,19] with a time step of $\Delta t = 0.002$ ps. To perform multi-particle solvent collisions, the simulation box was divided into $(32)^3$ cells. Multi-particle solvent collisions were carried out every 50 molecular dynamics time steps so that $\tau = 0.1$ ps. At these discrete time intervals, the velocities of all solvent particles in a frame moving with the velocity of the center of mass of the particles in each cell were rotated by $\pi/2$ along a randomly chosen direction independently in each cell.

3. Cluster structure and dynamics

Although isolated clusters are metastable, for some temperature ranges and potential parameters they can persist for long enough time periods so that their "equilibrium" properties can be established. For example, both Lennard–Jones and molecular clusters composed of tens to thousands of molecules have been investigated by simulation methods and have been shown to exist in a variety of thermodynamic states, including solid and liquid states [20–30]. In this section, we consider LJ clusters that exist in the liquid state in vacuum and examine how the structure and dynamics of the clusters changes when they are embedded in a mesoscopic solvent.

3.1. Cluster structure

We begin with a discussion of moderately large clusters with sizes of $M = 25$ and 123 particles (Fig. 1). At temperatures of $T = 40.33$ K ($T^* = 0.33$) and 48.4 K ($T^* = 0.4$),

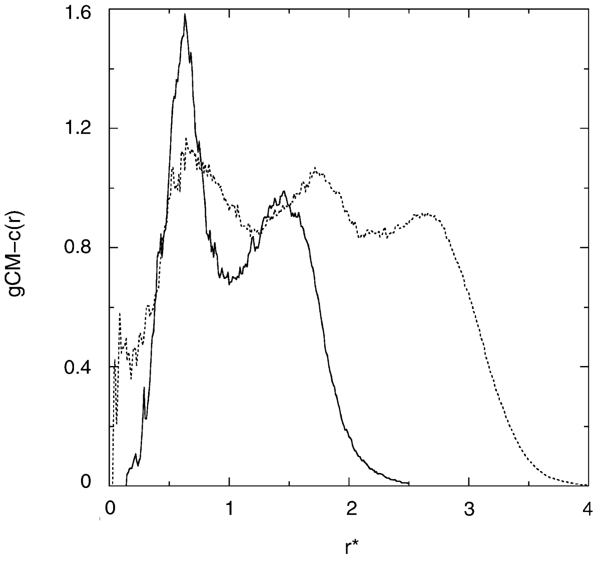

Fig. 1. Radial distribution function $g_{CM-c}(r)$ versus $r^* = r/\sigma_{cc}$ for $M = 25$ (solid line) and $M = 123$ (dotted line) clusters in vacuum.

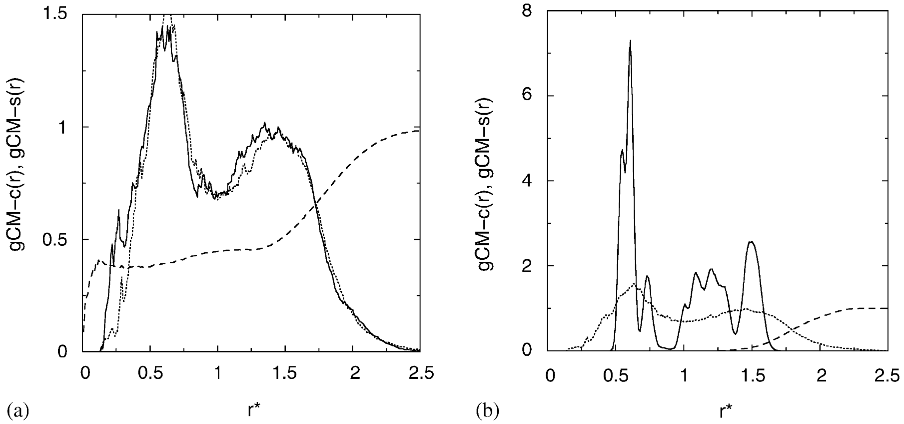

Fig. 2(a)–(b). Radial distribution function $g_{CM-c}(r)$ versus r^* for $\sigma_{cs} = 0.17$ nm (left) and $\sigma_{cs} = 0.221$ nm (right) for $M = 25$ clusters in the mesoscale solvent (solid lines); vacuum cluster (dotted lines). Also shown is the solvent radial distribution function $g_{CM-s}(r)$ (dashed lines).

respectively, these clusters exist in the liquid state and persist with little or no evaporation during the 1–2 ns of our simulations.

It is convenient to characterize the cluster structure in terms of the radial distribution functions for cluster and solvent molecules relative to the center of mass of the cluster. These distribution functions are defined by

$$g_{CM-\alpha}(r) = \frac{1}{4\pi r^2 \rho_\alpha} \left\langle \sum_i^{N_\alpha} \delta(|\mathbf{x}_i - \mathbf{R}_{CM}| - r) \right\rangle , \tag{9}$$

where $\alpha = c$ or s designates a cluster or solvent molecule, $\mathbf{R}_{CM}$ is the center of mass of the cluster and ρ_α is the number density of cluster or solvent molecules. In this expression, we take $\rho_c = \sigma_{cc}^{-3} = 25.44\ \text{nm}^{-3}$ and $\rho_s = 2035.42\ \text{nm}^{-3}$.

Fig. 1 shows this radial distribution function for two clusters in vacuum with $M = 25$ and 123 particles at temperatures of $T^* = 0.33$ and $T^* = 0.4$, respectively. The results were obtained by performing constant temperature MD simulations to thermalize the clusters at the desired temperature, followed by a 1–2 ns constant energy simulation to obtain the information needed to compute the radial distribution function. The graphs of $g_{CM-c}(r)$ show liquid-like distributions of cluster particles at these temperatures and structural ordering within the clusters. Two prominent cluster particle layers are seen in the $M = 25$ cluster and three prominent layers in the $M = 123$ particle cluster. Such structural features in large liquid LJ clusters have been seen in earlier investigations [24–26]. We have verified the liquid-like character of cluster by computing the mean-square displacement of the cluster particles.

Next, we consider the modifications in the cluster structure that occur when the clusters are embedded in the mesoscopic solvent. Since the solvent interacts with the cluster particles through repulsive intermolecular forces, we can study the modifications in the cluster structure and dynamics as a function the parameters in these interactions.

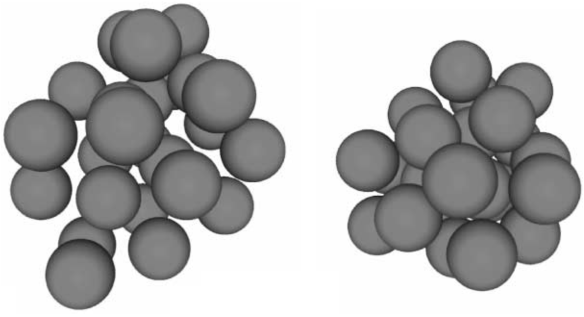

Fig. 3. Instantaneous cluster configurations for $M=25$ clusters with $\sigma_{cs}=0.17$ nm (left) and $\sigma_{cs}=0.221$ nm (right) showing the liquid-like and solid-like structures of these two cases. The solvent molecules are not shown in these figures.

Due to the mesoscopic treatment of the solvent, its equation of state is the ideal gas law in the absence of any embedded particles. The actual pressure felt by the cluster molecules depends on the cluster particle–solvent molecule interactions. In the calculations described below, we fix $\varepsilon_{cs}=\varepsilon_{ss}$ and vary σ_{cs}. The $M=25$ cluster radial distribution functions are shown in Figs. 2 (left) and (right) for $\sigma_{cs}=0.17$ nm and $\sigma_{cs}=0.221$ nm, respectively. These results may be compared with the corresponding vacuum values also shown in the figure. Also, in these figures we show the radial distribution functions $g_{CM-s}(r)$ for the solvent molecules relative to the cluster center of mass. The structures of the radial distribution functions are similar in vacuum and in the mesoscopic solvent for $\sigma_{cs}=0.17$ nm but considerable structural changes take place when $\sigma_{cs}=0.221$ nm. For $\sigma_{cs}=0.221$ nm the cluster is compressed and actually adopts a solid-like configuration. These differences are seen in cluster configurations drawn from the molecular dynamics simulation shown in Fig. 3.

The origin of this difference can be found in the structure of the solvent molecule–cluster particle distributions. For $\sigma_{cs}=0.17$ nm, the solvent molecules are able to penetrate into the cluster while for $\sigma_{cs}=0.221$ nm they are not able to do so. Consequently, in the latter case, the solvent provides a larger external force on the cluster which compresses it and induces a solid-like structural configuration.

The results presented in Fig. 4 for $g_{CM-c}(r)$ and $g_{CM-s}(r)$ for clusters with $M=123$ particles exhibit structural changes similar to those for the $M=25$ particle clusters. Again, for $\sigma_{cs}=0.17$ nm solvent molecules are able to penetrate into the cluster interior and cluster structure exhibits only small changes compared to that in its vacuum state. For $\sigma_{cs}=0.221$ nm, there is almost no penetration into the cluster by solvent molecules and the cluster adopts a solid-like structure.

For the large compact clusters considered above we have two situations. For $\sigma_{cs}=0.17$ nm solvent penetrates the cluster, however, the solvent molecules within the cluster cannot be regarded as a continuum since they are few in number and their dynamics is dominated by cluster particle–solvent molecule intermolecular forces. For $\sigma_{cs}=0.221$ nm solvent molecules are not able to penetrate into the interior of the

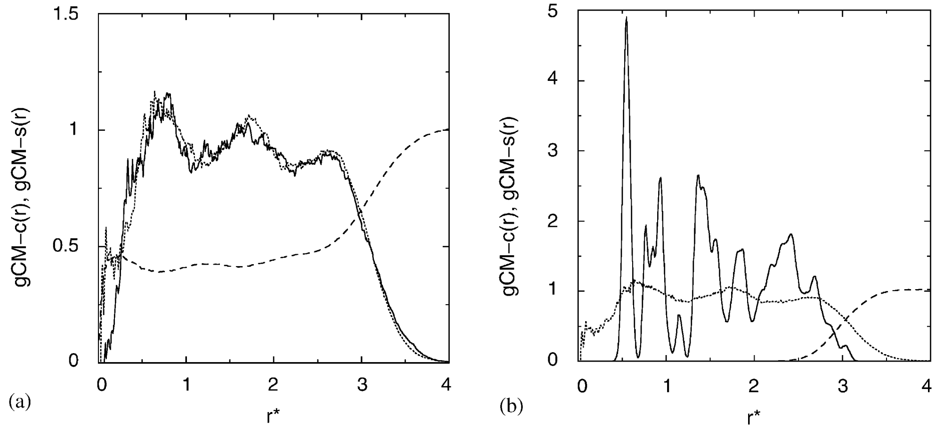

Fig. 4(a)–(b). Radial distribution function $g_{CM-c}(r)$ versus r^* for $\sigma_{cs} = 0.17$ nm (left) and $\sigma_{cs} = 0.221$ nm (right) for $M = 123$ clusters in the mesoscale solvent (solid lines); vacuum cluster (dotted lines). Also shown is the solvent radial distribution function $g_{CM-s}(r)$ (dashed lines).

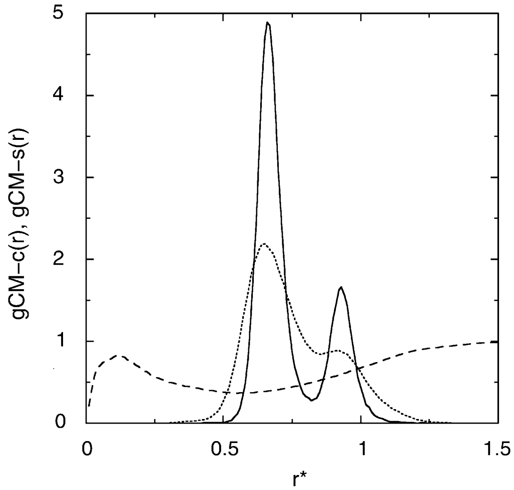

Fig. 5. Radial distribution function $g_{CM-c}(r)$ versus r^* for the LJ cluster with $M = 5$: vacuum cluster (dotted line); cluster in mesoscale solvent (solid line); solvent radial distribution function $g_{CM-s}(r)$ (dashed line).

cluster and the cluster structure is determined mainly by intermolecular forces at the cluster surface. Consequently, it is of interest to investigate the structure and dynamics of a small cluster where all cluster molecules are in close contact with the mesoscale solvent.

For this purpose we take $M = 5$ and LJ parameters $\varepsilon_{cc} = 5.0302$ kJ/mol and $\sigma_{cc} = 0.34$ nm. The mean kinetic energy of the particles was chosen to correspond to a cluster temperature of $T = 85$ K. For these parameters, this small cluster persists without evaporation for the duration of our simulations (1 ns) and is liquid-like. The radial distribution function $g_{CM-c}(r)$ is shown in Fig. 5 and displays two prominent peaks

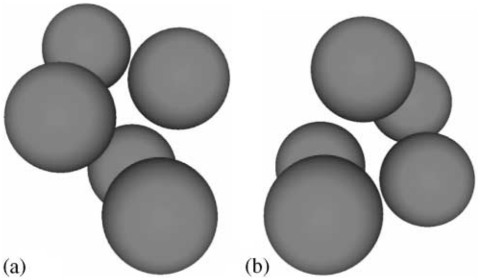

Fig. 6(a)–(b). Instantaneous cluster configurations for the $M = 5$ cluster; in mesoscopic solvent (left) and in vacuum (right).

reflecting the structural ordering in this small cluster. The peak at small r corresponds to two particles while that at larger r corresponds to three particles. Two cluster configurations drawn from the molecular dynamics simulation are shown in Fig. 6.

If this cluster is embedded in a mesoscopic solvent which interacts with the cluster particles through truncated LJ potentials with $\varepsilon_{cs} = 1.00604$ kJ/mol and $\sigma_{cs} = 0.17$ nm, the cluster structure and dynamics is modified. Fig. 5 compares the resulting cluster radial distribution with that for the vacuum cluster. The repulsive interactions with the solvent molecules have the effect of making the cluster more compact and increasing the structural ordering within the cluster as reflected in the more prominent peaks in g_{CM-c}. The solvent radial distribution function indicates that the solvent molecule density in the cluster particle vicinity is lower than that in the bulk of the solvent but nevertheless solvent molecules are found in significant numbers throughout the cluster—all cluster particles feel the influence of solvent molecules.

3.2. Cluster diffusion and dynamics

The vacuum clusters were prepared with no net translation of the center of mass of the cluster; however, in the presence of the solvent, the cluster as a whole may diffuse and this diffusion provides information on the interactions of the cluster with its environment. In general, one may expect that the diffusion of such complex molecular entities with internal dynamics will not be simple. Nevertheless, we shall show that simple hydrodynamic models, while unable to quantitatively characterize the diffusion coefficients, are able to capture some of their qualitative aspects.

The mean-square displacement of the center of mass of the cluster was found to vary linearly with time and the diffusion coefficients were extracted from this data. We use the notation $D_{CM}(M; \sigma_{cs})$ to label the various cluster diffusion coefficients since their values will depend on the cluster size and the nature of the interactions with the solvent. We find values of $D_{CM}(25; 0.17) = 9.6 \times 10^{-7}$ cm^2/s, $D_{CM}(25; 0.221) = 1.3 \times 10^{-6}$ cm^2/s, $D_{CM}(123; 0.17) = 3.9 \times 10^{-7}$ cm^2/s, $D_{CM}(123; 0.221) = 4.3 \times 10^{-7}$ cm^2/s, and $D_{CM}(5; 0.17) = 5.7 \times 10^{-6}$ cm^2/s.

The large compact clusters with $M = 25$ and 123 will appear as rough nearly spherical objects to the mesoscopic solvent and on large enough scales the interactions with the solvent should be mimicked by stick boundary conditions at the cluster surfaces to the surrounding fluid with viscosity η. Consequently, in this large particle limit, one might expect the diffusion coefficient to be given approximately by the Stokes–Einstein relation:

$$D_{SE} = \frac{k_B T}{6\pi\eta R_c} , \tag{10}$$

where R_c is the radius of the cluster.

We use the notation $R_c(M;\sigma_{cs})$ to denote the dependence of R_c on the cluster size and σ_{cs} values. From the radial distribution function data one may obtain crude estimates of the cluster sizes and we find $R_c(25;0.17) \approx 2.25$, $R_c(25;0.221) \approx 1.6$, $R_c(123;0.17) \approx 3.5$, $R_c(123;0.221) \approx 3.0$ and $R_c(5;0.17) \approx 1.0$ in units of σ_{cc}. The viscosities of the bulk mesoscopic solvent may be obtained by direct simulation of the autocorrelation expressions for the viscosity [13]. We find the values $\eta(25) = 5.0 \times 10^{-4}$ N s/m^2, $\eta(123) = 6.5 \times 10^{-4}$ N s/m^2 and $\eta(5) = 1.0 \times 10^{-3}$ N s/m^2 for the viscosities appropriate for the three cluster cases studied here. (The viscosities are labeled by the cluster size M although the viscosity is that for the bulk solvent in the absence of a cluster. This notation is used since the temperature of the system is different for different cluster sizes and this affects the value of the viscosity.)

Using these values of the radii and viscosities in the Stokes–Einstein relation for the diffusion coefficient, we find $D_{SE}(25;0.17) = 7.8 \times 10^{-7}$ cm^2/s, $D_{SE}(25;0.221) = 1.1 \times 10^{-6}$ cm^2/s, $D_{SE}(123;0.17) = 4.6 \times 10^{-7}$ cm^2/s, $D_{SE}(123;0.221) = 5.4 \times 10^{-7}$ cm^2/s and $D_{SE}(5;0.17) = 1.8 \times 10^{-6}$ cm^2/s. These results should be compared to the values extracted from the mean square displacements of the centers of mass of the clusters. The results are in qualitative agreement although there are quantitative discrepancies. Such differences are to be expected in view of the fact that the clusters are not macroscopic objects and cluster molecules interact with the solvent via intermolecular forces so the radii to be used in the Stokes–Einstein relation are not precisely determined. In addition, the clusters are not simple spheres but have internal structure and dynamics. Note that for $M = 5$ where such a model is expected to have the least validity the result is much farther from the Stokes–Einstein value but still reflects the large hydrodynamic contribution to the diffusion coefficient. (See Ref. [10] for a discussion of microscopic and hydrodynamic contributions to the diffusion coefficient.)

For the larger clusters the general trends in the diffusion data are in accord with the simple scaling predicted by the Stokes–Einstein law for the larger clusters. The ratios of the diffusion coefficients should be inversely related to the ratio of the cluster radii if the Stokes–Einstein relation is valid. We have $D_{CM}(25;0.221)/D_{CM}(25;0.17) \approx 1.35$ while $R_c(25;0.17)/R_c(25;0.221) \approx 1.4$. For the larger $M = 123$ cluster we have $D_{CM}(123;0.221)/D_{CM}(123;0.17) \approx 1.1$ while $R_c(123;0.17)/R_c(123;0.221) \approx 1.2$. These results confirm that the mesoscopic solvent acts like hydrodynamic continuum on large distance and time scales and is able to reproduce the hydrodynamic effects responsible for the diffusive motion.

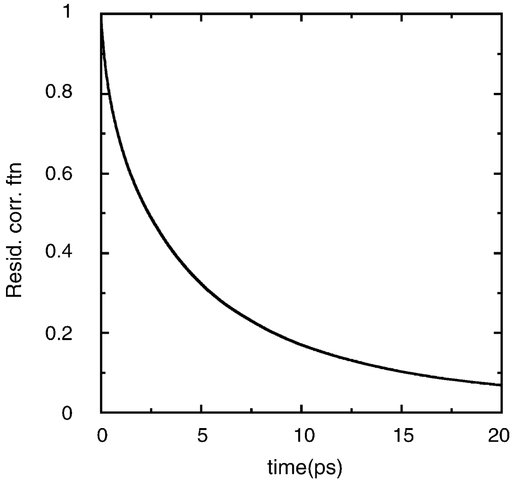

Fig. 7. Residence time correlation function $\mathscr{C}_s(t)$ versus time for the $M = 25$ particle cluster with $\sigma_{cs} = 0.17$.

It is interesting to study the dynamics of the solvent molecules that penetrate into the cluster interiors for $\sigma_{cs} = 0.17$. To investigate the dynamics of these trapped solvent molecules, we have computed their mean residence time within the cluster in the following way. Let $\theta(R_c - |\mathbf{r}_i(t) - \mathbf{R}_{CM}|)$ be the characteristic function which is unity if the solvent particle i is within the cluster with radius R_c at time t and zero otherwise. The residence time correlation function is defined as

$$\mathscr{C}_s(t) = \mathscr{N}_s^{-1} \sum_{i=1}^{N_s} \langle \theta(R_c - |\mathbf{r}_i(t) - \mathbf{R}_{CM}|)\theta(R_c - |\mathbf{r}_i(0) - \mathbf{R}_{CM}|) \rangle \,, \qquad (11)$$

where $\mathscr{N}_s$ is the average number of solvent molecules in the cluster at time zero and the angle brackets signify an average over realizations of the cluster preparation. A plot of $\mathscr{C}_s(t)$ versus t is shown in Fig. 7. The residence time extracted from this exponential decay is $\tau_R(25; 0.17) = 8.33$ ps. The decay in Fig. 7 and the value of the mean residence time provide information on the nature of the diffusive escape of a collection of small molecules from a compact, dynamic collection of large scatterers.

4. Conclusion

The results of this investigation have shown that the hybrid molecular dynamics–mesoscopic solvent dynamics model provides a route for the description of the structural modifications and dynamics of large molecular entities in a fluid environment. Specific structural modifications were seen to arise from the variations of the mesoscopic solvent–solute particle interactions. In dealing with large molecules in various types of solvent environments, such as polar or non-polar, hydrophobic or hydrophilic interactions, molecular structural changes will occur as a result of the specific nature of these interactions. However, the large scale motions of these groups are likely to be governed by the hydrodynamic fields of the surrounding solvent rather than these specific interactions. For the relatively simple cluster systems considered here we have shown that both these effects can be captured by the hybrid model with a mesoscopic treatment of the solvent.

As a result of the solvent–solute molecule interactions, the solvent structure is also non-trivial in the vicinity of the solute molecules. However, because of the manner in which the solvent dynamics is carried out solvent–solvent structural features are absent—the equation of state for the fluid solvent alone is that of an ideal gas. Consequently, the solvent structural correlations in the vicinity of the solvent reflect only the solvent–solute interactions and are, therefore, not completely correct. The extent to which such correlations may be neglected depends on the application. The extension of the hybrid model to incorporate such structural effects in the vicinity of the solute remains a topic for research.

The results presented here suggest that the combination of full molecular dynamics for certain species embedded in a fluid which is treated at a mesoscopic level is a fruitful way to treat aspects of the structure and dynamics that goes beyond simple hydrodynamic and Langevin descriptions. This method could find application in the study of a variety of chemical rate processes involving large scale conformational changes and other problems in biological and microcolloidal dynamics.

Acknowledgements

This work was supported in part by a grant from the Natural Sciences and Engineering Research Council of Canada. The work of S.H.L. was supported by a Korea Research Foundation Grant (KRF-2001-015-DP0215).

References

[1] G.K. Batchelor, An Introduction to Fluid Mechanics, Cambridge University Press, Cambridge, 1970.
[2] L.D. Landau, E.M. Lifshitz, Fluid Mechanics, Pergamon Press, New York, 1959.
[3] D. Bedeaux, P. Mazur, Physica A 73 (1974) 287.
[4] J. Happel, H. Brenner, Low Reynolds Number Hydrodynamics, Noordhoff International Publishing, Leyden, 1973.
[5] P. Mazur, Physica A 110 (1982) 128.
[6] P. Mazur, W. van Saarloos, Physica A 115 (1982) 21.
[7] C.W.J. Beenakker, P. Mazur, Physica A 120 (1983) 388.
[8] B.U. Felderhof, J. Phys. A 11 (1978) 929.
[9] B.J. Alder, T.E. Wainwright, Phys. Rev. Lett. 18 (1967) 988.
[10] J.T. Hynes, R. Kapral, M. Weinberg, J. Chem. Phys. 70 (1979) 1456.
[11] J.M. Deutch, I. Oppenheim, J. Chem. Phys. 54 (1971) 3547.
[12] M. Tokuyama, I. Oppenheim, Physica A 94 (1978) 501.
[13] A. Malevanets, R. Kapral, J. Chem. Phys. 110 (1999) 8605.
[14] G.A. Bird, Molecular Gas Dynamics, Clarendon Press, Oxford, 1976.
[15] G.A. Bird, Comp. Math. Appl. 35 (1998) 1.

[16] A. Malevanets, R. Kapral, J. Chem. Phys. 112 (2000) 7260.
[17] A. Malevanets, J. Yeomans, Europhys. Lett. 52 (2000) 231.
[18] W.C. Swope, H.C. Andersen, P.H. Berens, K.R. Wilson, J. Chem. Phys. 76 (1982) 673.
[19] M. Tuckerman, B.J. Berne, G.J. Martyna, J. Chem. Phys. 97 (1992) 1990.
[20] R.S. Berry, T.L. Beck, H.I. Davis, J. Jellinek, Adv. Chem. Phys. 70 (1988) 75.
[21] M.Y. Hahn, R.L. Whetten, Phys. Rev. Lett. 61 (1988) 1190.
[22] H.-P. Cheng, X. Li, R.L. Whetten, R.S. Berry, Phys. Rev. A 46 (1992) 791.
[23] J.D. Honeycutt, H.C. Andersen, J. Phys. Chem. 91 (1987) 4950.
[24] B.G. Moore, A.A. Al-Quraishi, Chem. Phys. 252 (2000) 337.
[25] A.S. Clarke, R. Kapral, B. Moore, G. Patey, X.-G. Wu, Phys. Rev. Lett. 70 (1993) 3283.
[26] A.S. Clarke, R. Kapral, G. Patey, J. Chem. Phys. 101 (1994) 2432.
[27] A.W. Castleman Jr., R.G. Keese, Chem. Rev. 86 (1986) 589.
[28] A.W. Castleman Jr., R.G. Keese, Annu. Rev. Phys. Chem. 37 (1986) 525.
[29] A.W. Castleman Jr., R.G. Keese, Science 241 (1988) 36.
[30] A.W. Castleman Jr., S. Wei, Annu. Rev. Phys. Chem. 45 (1994) 685.